Role of Catalytic Residues in Enzymatic Mechanisms of Homologous Ketosteroid Isomerases[†,‡]

Kyung Seok Oh,[§] Sun-Shin Cha,[||] Do-Hyung Kim,[§,||] Hyun-Soo Cho,[||] Nam-Chul Ha,[||] Gildon Choi,[||] Jin Yong Lee,[§] P. Tarakeshwar,[§] Hyeon S. Son,[§] Kwan Yong Choi,*[,||] Byung-Ha Oh,*[,||] and Kwang S. Kim*[,§]

National Creative Research Initiative Center for Superfunctional Materials, Department of Chemistry and Department of Life Science, Division of Molecular and Life Sciences, Pohang University of Science and Technology, San 31, Hyojadong, Namgu, Pohang 790-784, Korea

Received July 12, 2000; Revised Manuscript Received August 28, 2000

ABSTRACT: Ketosteroid isomerase (KSI) is one of the most proficient enzymes catalyzing an allylic isomerization reaction at a diffusion-controlled rate. In this study of KSI, we have detailed the structures of its active site, the role of various catalytic residues, and have explained the origin of the its fast reactivity by carrying out a detailed investigation of the enzymatic reaction mechanism. This investigation included the X-ray determination of 15 crystal structures of two homologous enzymes in free and complexed states (with inhibitors) and extensive ab initio calculations of the interactions between the active sites and the reaction intermediates. The catalytic residues, through short strong hydrogen bonds, play the role of charge buffer to stabilize the negative charge built up on the intermediates in the course of the reaction. The hydrogen bond distances in the intermediate analogues are found to be about 0.2 Å shorter in the product analogues both experimentally and theoretically.

Ketosteroid isomerase (KSI),[1] which catalyzes the conversion of β,γ- to α,β-unsaturated steroidal ketones via a dienol(ate) intermediate at a nearly diffusion-controlled rate (Scheme 1), is a paradigm for fast enzymatic reactions (*1*). Two homologous bacterial enzymes are known: *Pseudomonas testosteroni* (TI) and *Pseudomonas putida* (PI). KSI involves metabolites of steroid compounds, and in mammals, the enzyme activity is essential for the synthesis of steroid hormones. Site-directed mutagenesis and structural analysis of KSI indicate that Asp38 serves as a base for abstracting the C4β-proton of the steroid substrate, while Tyr14 (hydrogen bonded to Tyr55) and Asp99 serve as catalytic residues[2] by providing hydrogen bonds to the oxyanion

Scheme 1

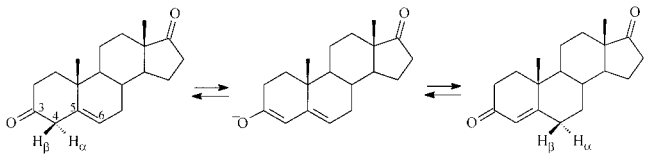

(C3−O or O3) of the dienolate intermediate (*2*−*7*). Tyr14 has been proposed to form a short strong hydrogen bond (SSHB) with the reaction intermediate (*8*, *9*). The replacement of Tyr14 by phenylalanine decreases k_{cat} by $10^{4.7}$-fold, which corresponds to the stabilization of the transition state by 6.4 kcal/mol (*10*). The comparison of the dissociation rate constants of the intermediate gives 7.6 kcal/mol for the stabilization energy by Tyr14 (*11*, *12*). Most of the stabilization can be attributed to the formation of the strong hydrogen bond. Evidence for this strong hydrogen bond emerges from the pK_a of 11.6 of Tyr14, which is close to its value of 10.0 in the dienol (*13*). KSI also exhibits unusually deshielded ^{1}H resonance characteristics of SSHB upon binding reaction intermediate analogues such as dihydroxyequilenin, equilenin, or estradiol 17β-hemisuccinate (*14*−*16*). Despite these supporting evidence, the exact role of SSHB in KSI has not been established clearly.

Although the existence of SSHB has been realized for a long time (*17*, *18*), the proposal by Gerlt and Gassman (*8*) and Cleland and Kreevoy (*19*), that SSHBs play a key role in enzyme catalysis, has been a highly debated issue in recent years (*20*−*22*). SSHBs are distinguished from normal hydrogen bonds by their large hydrogen bond energies (10−20 kcal mol^{-1}), short distances, and large downfield shift of NMR resonances. In low dielectric organic solvents, unusual physicochemical properties have been observed for a number

[†] This study was supported by Creative Research Initiatives (KISTEP) of Korea Ministry of Science and Technology, and Korea Science and Engineering Foundation Grant 98-0401-04-01-5, and in part by the Brain Korea 21 Project.

[‡] This study used the X-ray Facility at Pohang Light Source. The atomic coordinates (code 1QJG) have been deposited with the Protein Data Bank, Research Collaboratory for Structural Bioinformatics, Rutgers University, New Brunswick, NJ.

* To whom correspondence should be addressed. (K.S.K.) Phone: +81-54-279-2110. Fax: +82-54-279-8137. E-mail: kim@postech.ac.kr. (B.H.O.) Phone: +81-54-279-2289. Fax: +82-54-279-2199. E-mail: bhoh@postech.ac.kr. (K.Y.C.) Phone: +81-54-279-2295. Fax: +82-54-279-2199. E-mail: kchoi@postech.ac.kr.

[§] National Creative Research Initiative Center for Superfunctional Materials.

[||] Department of Life Science.

[1] Abbreviations: KSI, ketosteroid isomerase; H-bond, hydrogen bond; SSHB, short strong hydrogen bond; PI, *Pseudomonas putida* KSI; TI, testosteroni KSI; ES, enzyme−substrate complex; EP, enzyme−product complex; EI, enzyme intermediate state; TS, transition state; HOMO, highest occupied molecular orbital.

[2] We used the residue-numbering convention for TI. In case of PI, the residue numbers of the catalytic residues are Asp40, Tyr16, (Tyr57), and Asp103.

10.1021/bi001629h CCC: $19.00
Published on Web 10/21/2000

Table 1: Structure Determination and Crystallographic Statistics

	D38N:estrone	WT:equilenin	D38N:testosterone
source	CuKα	CuKα	CuKα
wavelength (Å)	1.5418	1.5418	1.5418
resolution range (Å)	20.0−1.8	20.0−1.9	20.0−2.3
R_{sym} (%)[a]	4.0	5.3	7.0
completeness (>1σ, %)	90.7	89.7	88.1
(outer shell)	(79.3)	(80.4)	(78.33
R-factor/R_{free} (>1σ, %)[b]	21.1/25.6	20.7/25.6	20.5/26.1
rmsd bond length (Å)	0.009	0.009	0.008
rmsd bond angle (deg)	1.356	1.382	1.241
Ramachandran plot (%)			
most favored region	89.9	88.8	87.8
additionally allowed region	10.1	11.2	12.3

[a] $R_{sym} = \sum|I_{obs} - I_{avg}|/\sum I_{obs}$. [b] R-factor $= \sum||F_O| - |F_C|/\sum|F_C|$, where $|F_O|$ and $|F_C|$ are the observed and calculated structure factor amplitudes, respectively. R_{free} was calculated with 5% of the data.

of hydrogen bonds between two partners with an equal pK_a (*23*). These include highly deshielded ^{1}H nuclear magnetic resonance (NMR) observed at higher than 16 ppm (*16*, *24*, *25*), low isotopic fractionation factors (*26*), and isotope effects on infrared stretching frequencies (*17*). An elucidation of the role of SSHBs in stabilizing highly reactive intermediates bound to the active site and accelerating the reaction rate is of importance in understanding the catalytic mechanism of a large class of enzymes involving carbanions. Therefore, we have investigated the structure of the active site of KSI using both X-ray analysis and ab initio theoretical methods.

Previously, only two key catalytic residues of Asp38 and Tyr14 were known (*11*, *12*). A recent NMR study of Pollack and co-workers, however, indicated the involvement of three key catalytic residues (Asp38, Asp99, and Tyr14) (*5*, *27*). This is readily supported by the X-ray structure of PI in complex with equilenin (a reaction intermediate analogue) by Oh and co-workers (*6*, *16*). Tyr14 and Asp99 are H-bonded to the C3−O of equilenin (O3), and Asp38 is in the proximity of C4 and C6 of equilenin. An ancillary residue Tyr55 is H-bonded to Tyr-14. (The presence of both Tyr14 and Tyr55 is denoted as Tyr14/55.) On the other hand, a recent NMR study carried out in solution indicates that Asp99 and equilenin-O3 are linked to Tyr14 (*28*, *29*). Thus the solution structure is dyadic with respect to Tyr14, which is in contrast to the X-ray crystal structure. The structure of the active site is essential in the investigation of the catalytic mechanism. X-ray structures of PI and TI in complex and the mutated D38N structure were reported in a recent study at 2.5 and 2.3 Å resolution, respectively (*6*, *7*). The crystal structures revealed that the hydrogen bond between Tyr14 and the dienolic intermediate is short. Here we report further refined structures in various conditions to emphasize that the short H-bonds have a vital role in the intermediate states.

On a parallel note, the recent ab initio calculations of Kim et al. have highlighted the role of the short hydrogen bond between Tyr14 and Asp99 in the elucidation of the catalytic mechanism of KSI (*30*). Their dissection of the energy profile into the various factors responsible for the reaction mechanism indicated that a significant stabilization resulted from the formation of a hydrogen bond between Tyr14 and Asp99. This comparison of the theoretically predicted hydrogen bonds with those of the highly refined X-ray structures enables us to provide solutions to three controversial issues: (i) the possible difference between the active site structures of the crystal and solution phases, (ii) the role of each catalytic residue in the enzymatic reactions, and (iii) the role of SSHBs in the diffusion controlled reaction.

EXPERIMENTAL PROCEDURES

Materials. Equilenin and estrone were purchased from Steraloids. Testosterone was purchased from Sigma. Superose 12 gel filtration column was obtained from Amersham Pharmacia Biotech.

Mutant Construction and Protein Purification. Wild-type and mutant enzymes were overexpressed from *Escherichia coli* [BL21 (DE3)], and purified by a deoxycholate affinity chromatography and Superose 12 gel filtration chromatography as described previously (*31*, *32*). All mutant enzymes contain the D38N mutation to achieve tighter binding of steroids to the enzymes. This is because of the absence of the negative charge at residue 38 (*33*).

Crystallization. Crystallization of the enzymes in complex with equilenin, an intermediate analogue, was accomplished by procedures described previously albeit with a slight modification (*7*). The enzyme solution was prepared at 20 mg/mL concentration in 50 mM Tris-Cl, pH 7.0, containing 20 mM β-mercaptoethanol, and 70 μL of this solution was mixed with 2 μL of equilenin in dimethyl sulfoxide. The crystals of the complex were grown from 1.1 M ammonium acetate and 0.1 M sodium acetate, pH 4.6, by the hanging drop vapor diffusion method at 22 °C. The resulting crystals belong to the C2 space group with unit cell dimensions of $a = 88.41$, $b = 73.17$, $c = 51.52$, and $\beta = 90.33$. The detailed information on the crystals of the enzymes complexed with equilenin are presented in Table 1.

Data Collection, Structure Determination, and Refinement. Diffraction data for all but one, D38N/Y14F−PI:equilenin complex, were measured on a DIP2020 area detector with graphite monochromated CuKα X-rays generated by a MacScience M18XHF rotating anode generator operated at 90 mA and 50 kV at room temperature. Only small crystals of D38N/Y14F−PI:equilenin complex were obtained, grown out of heavily precipitated proteins. The data for the complex were collected using BL18B beamline at Photon Factory, Japan. Data reduction, merging, and scaling were accomplished with the programs DENZO and SCALEPACK (*34*). The structure of KSI−inhibitor complexes were solved by the molecular replacement protocol in the X-PLOR suite of programs (*35*) using the dimeric structure of the unin-

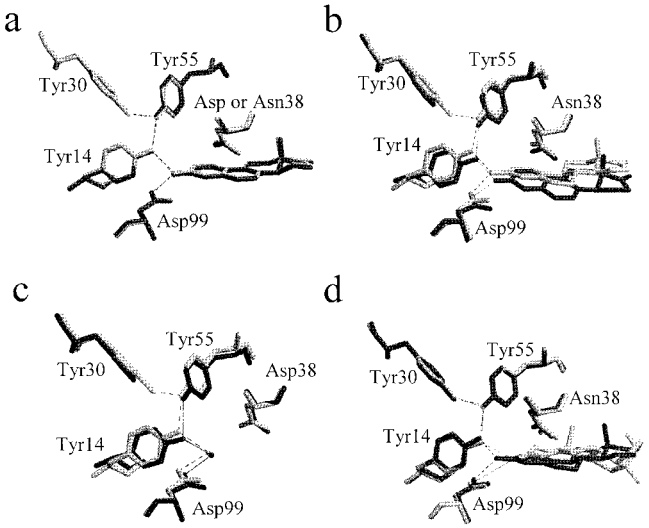

FIGURE 1: Superposed X-ray structures of active sites of PI/equilenin (in black) and PI(D38N)/equilenin (in gray) (1.9 and 2.1 Å resolutions, respectively) (a), TI(D38N)/equilenin (in black) and PI(D38N)/estrone (in gray) and (2.3 and 1.8 Å resolutions) (b), PI/water (in black) and TI/water (in gray) (1.9 and 2.3 Å resolutions) (c), and PI(D38N)/estrone (in black) and PI(D38N)/testosterone (in gray) (1.8 and 2.3 Å resolutions) (d).

hibited enzyme (*6*). The statistics for the final structures are shown in Table 1.

Ab Initio Calculations. Calculations of energetics by full geometry optimization without constraints were done using Becke's three parameters with Lee−Yang−Parr density functionals (B3LYP) and the 6-31+G* basis set using a Gaussian 94 suite (*36*). All the minimum and transition-state geometries were confirmed by the vibrational frequency analysis at the Hartree−Fock level employing 3-21G basis set. The entropy effects were investigated using these vibrational frequencies. This effect was found to be insignificant (within only ∼2 kcal/mol), so this discussion is omitted in this paper. In the calculation, Asp38, Asp99, Tyr14, Tyr55, equilenin, and steroid were replaced by formate, formic acid, phenol, methanol, 2-naphthol, and β,γ-enone derivative, respectively. Further refined energies were calculated by using the self-consistent-reaction field [dielectric constant $\epsilon = 18$ (13)], employing Moller−Plesset second-order perturbation theory with 6-31+G* basis set [SCRF-(MP2)/6-31+G*] at the B3LYP/6-31+G* optimized geometries.

RESULTS AND DISCUSSION

Active-Site Geometry. Previously, the crystal structures of PI or TI in complex with equilenin as intermediate analogues were obtained with mutation of D38N at somewhat low resolution. Here, we obtained various X-ray structures at higher resolution. A refined X-ray structure of the PI-(D38N)−equilenin complex has been obtained at 2.1 Å resolution [in contrast to the previous 2.5 Å resolution (*6*)]. This refined structure of the intermediate analogue is compared with a new X-ray structure of PI−equilenin complex (without mutation of D38N) obtained at 1.9 Å resolution in Figure 1a. The structure of PI(D38N) in complex with estrone has been determined at 1.8 Å resolution, which is the best refined structure among the 15 structures (of PI, TI, and the mutants in free or in complex with inhibitors) investigated so far. This highly refined active site structure has been compared to that of the TI(D38N)-equilenin structure (2.3 Å resolution) in Figure 1b. In addition, the crystal structure of PI(D38N/D99L) in complex with equilenin has been obtained at 1.9 Å resolution (which is not shown here). In Figure 1c, we compare the active-site structures of PI and TI which interact with water molecules instead of substrates (1.9 and 2.3 Å resolutions, respectively) (*6*, *7*).

To compare the difference in structure between the intermediate and product analogues, we obtained the structure of PI(D38N) in complex with a product analogue, testosterone, at 2.3 Å resolution. This structure is compared with the most refined intermediate analogue structure of PI(D38N) in complex with estrone in Figure 1d. From these figures, it is clear that the active-site structures are almost similar regardless of the presence or absence of inhibitors. However, in the structures of the active sites in complex with the intermediate analogues, the hydrogen bond distances between O3 and Ty14 or Asp99 are ∼2.6 Å, which is slightly shorter (by ∼0.2 Å) than those (∼2.8 Å) of the structure in complex with the product analogue. It should be noted that some uncertainty exists in the experimental values. These results imply that Asp99 Oδ2 as well as Tyr14 OH may form a SSHB with steroid-O3 in the intermediate state of the active site of KSI. We find that the structures of the active site for 15 different crystals are essentially the same except for slight side-chain rotations due to the presence of void space. In consideration of similar bond distances for 15 crystal structures of KSI, the statistical errors in hydrogen bond distances from the O3 to the oxygen atoms of Tyr14 and Asp99 are estimated to be only ∼0.1 Å. Furthermore, the temperature factors of the atoms in the active site are much smaller than the average value of all atoms, indicating that the bond distance errors in the active site would be much smaller than the average error. NMR spectroscopic investigations also indicate that in the D38N mutant KSI, the H-bond between the catalytic residues and equilenin exhibits a large downfield shifted peak (>16 ppm) (*5*, *9*, *13*, *15*), which also implies the existence of SSHBs.

We find no significant difference in electron density between the wild-type and the mutants with D99L or Y14F substitution. However, in the structure of Y14F/D38N-equilenin, the inhibitor was bound "backward" with the steroid D-ring approaching Phe14. This might be due to the low affinity of the steroid toward the enzyme. The low affinity would indicate that the binding between Tyr14 and steroid-O3 might be stronger than that between Asp99 and steroid-O3. Actually, K_D for equilenin was very high when it was measured by fluorescence quenching analysis.

In the active-site environment of KSI, the two hydrogen bonds of Tyr-14 and Asp-99 with the substrate are completely surrounded by 22 apolar side chains. This excludes the ancillary residue Tyr55 which forms a hydrogen bond with Tyr14 OH and another ancillary residue Tyr30 which forms a H-bond with Tyr55 OH in case of PI, but not in TI. In particular, Val18, Phe82, and Val97 are purely apolar residues, which block the access of solvent molecules in the proximity of the oxyanion of the substrate. All the polar residues in the active site are surrounded by apolar amino acids and blocked from bulk solvent, resulting in zero water accessibility.

In the recent ab initio calculations of Kim et al. of the systems mimicking the active-site structures of the mutant enzymes with the catalytic residues Asp38, Tyr14, Asp99, and Tyr55, and with steroids (*30*), all the structures were fully optimized without constraints and the predicted structures were found to be in good agreement with the crystal structures. All these structures confirmed the presence of two hydrogen bonds having short distances between O3 and the oxygen atoms of residues O_r [$d(O_3-O_r)$], implying the possible existence of SSHBs. An analysis of the ab initio calculations revealed that the predicted active-site structures of KSI are very close to the X-ray structures. The predicted distances of $d(O_3-O_{Y14})$, $d(O_3-O_{D99})$, and $d(O_{Y14}-O_{D99})$ are 2.57, 2.54, and 4.19 Å in KSI/steroid, and 2.53, 2.55, and 4.01 Å in KSI/equilenin. These are in good agreement with the refined X-ray values: PI(D38N)/estrone at 1.8 Å resolution (2.58, 2.64, 4.02 Å), PI(D38N)/equilenin at 2.1 Å resolution (2.55, 2.59, 4.08 Å), PI/equilenin at 1.9 Å resolution (2.67, 2.49, 4.02 Å), and TI(D38N)/equilenin at 2.3 Å resolution (2.68, 2.54, 4.12 Å). In case of free enzyme PI/water, the three distances (where O_r is replaced by the water O atom) are (2.76, 3.36, 4.08 Å) at 1.9 Å resolution. Thus, the inter-oxygen distances are slightly increased.

Instead of the above O3-dyadic structures, we have also carried out the same level ab initio calculations for systems mimicking the Tyr14−diadic active-site structures (*28*). For this dyadic structure, the ab initio predicted distances are 2.67, 4.21, and 2.61 Å, which are quite off from the NMR-predicted distances of 2.72, 3.25, and 2.49 Å (*28*). Nevertheless, it can be seen that both the O3−dyadic and Tyr14−diadic structures have practically the same energies as the reactants of enzyme−substrate (ES) complexes. However, at the first enzyme−intermediate complex (EI1) states the O3−dyadic structure is 1.4 kcal/mol lower in energy than the Tyr14−diadic structure. All the above results indicate that the active-site structure in solution cannot be significantly different from those in the crystal structure. In the presence of product-like testosterone, the distances of $d(O_3-O_{Y14})$ and $d(O_3-O_{D99})$ are 2.78 and 2.81 Å at 1.9 Å resolution. This is in good agreement with the calculated product structure of steroid interacting with Tyr14, Asp99, and Asp38, and Tyr55, wherein the two distances are 2.71 and 2.67 Å. It should be noted from the X-ray structures that the distance $d(O_3-O_r)$ of the intermediate-like structure is ∼0.2 Å smaller than that of the product-like structure, in agreement with our previous prediction of the KSI-steroid structures along the reaction path (*30*).

Role of Catalytic Residues. The structural perturbation of the active-site geometry by mutation makes it hard to quantify the catalytic effect of the hydrogen bonds of Tyr14 and Asp99. Therefore, Kim and co-workers (*30*) have employed ab initio theoretical approaches to understand the roles of the hydrogen bonds by Tyr14 or Asp99 in catalysis (*30*). The predicted reaction constants (k_{cat}s) were in good agreement with the experimental values (*31*−*32*, *37*). Then, the two-step reaction mechanism was proposed to play an important role in enzymatic reaction in KSI (*30*). A couple of years back Mildvan and co-workers, based on NMR investigations, suggested that the dielectric constant (ϵ) of the enzymatic active site is 18, even though the active site is totally surrounded by apolar molecules. Since small changes in dielectric constant also affect the strength and

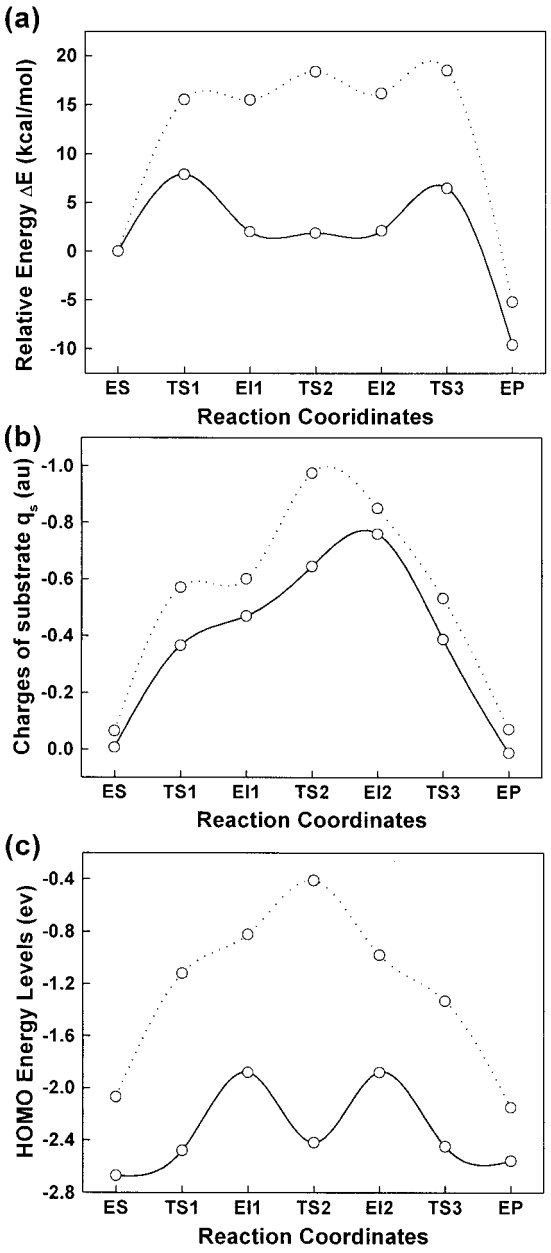

FIGURE 2: Predicted energy profiles (ΔE) along the reaction path for the Minimal and wild-type systems (a), the negative charge-build-up in the substrate (q_s in au) (b), and the HOMO energy levels (in eV) (c). The dotted and solid lines denote the minimal and wild-type systems, respectively.

formation of H-bonds, the theoretical results in this study have been obtained using a dielectric constant ($\epsilon = 18$). Figure 2a shows calculated energy profiles for the wild-type system (composed of Tyr14 and Asp99 as well as Asp38) and Minimal system (which has no assisting catalytic residue except for Asp38) in the medium [dielectric constant $\epsilon = 18$ (*13*)], which is in contrast to the previous energy profile for $\epsilon = 1$ (*30*). Here, we compare the energy profile with the charges of the substrate (Figure 2b) and the energy levels of the highest occupied molecular orbitals (HOMOs) (Figure 2c) along the reaction paths.

The energy profiles show three reaction steps from the enzyme−substrate complexes (ES) to the enzyme−product complex (EP) via the enzyme-transition state complexes (TSs) and the enzyme−intermediate complexes (EIs). EP has slightly lower energy than ES, consistent with the energy

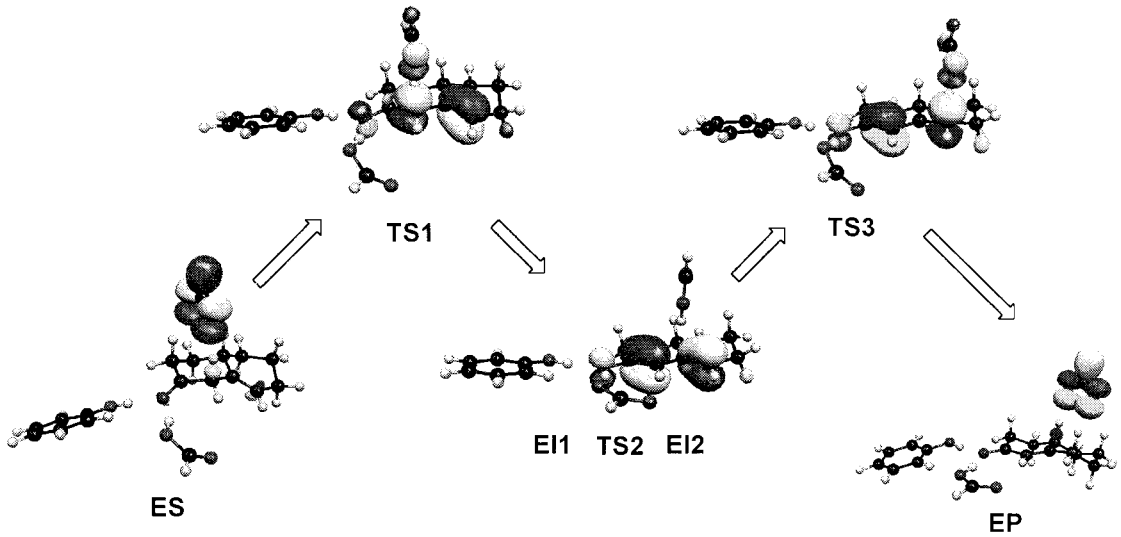

FIGURE 3: Electron density maps of the HOMO of the wild-type system representing the charge transfer from the Asp38 to substrate to catalytic residues (Tyr14 and Asp99) and back to the substrate along the reaction paths (from EI to EP via TSs and EIs).

profile obtained experimentally (*38*). The energy profile of the wild-type system shows that the barriers for the first (ES → TS1 → EI1) and the third (EI2 → TS3 → EP) steps are very similar in energy, while the second (EI1 → TS2 → EI2) step involving a small H-atom shift and a slight rotation about the C−C bond of Asp38 is not a rate-determining step. Hence, the reaction in the presence of catalytic residues can be essentially a two-step mechanism. In the wild type, TSs and EIs are 15−18 kcal/mol lower than ES in energy than the Minimal case without catalytic residues except for Asp38. In the presence of Tyr14 or Asp99, TS1 and TS3 are lowered by ∼6 kcal/mol than the minimal case. This result implies that the catalytic effect of the two residues is almost equivalent. When Tyr and Asp were introduced simultaneously, TS1 and TS3 were lowered by ∼10 kcal/mol. EIs and TS2 were stabilized by ∼15 kcal/mol, suggesting that the two functional groups contribute cooperatively to the stabilization of EIs and TS2.

As shown in Figure 2b, in the minimal case, the charge density in the frontier molecular orbitals found around the O3, shows a large build-up of negative charge on the substrate. In the case of the wild-type, the absolute charge of O3 is increased due to the presence of H atoms of the catalytic residues, which results in the strengthened hydrogen bonds toward SSHBs. Nevertheless, a portion of the charge density in the frontier molecular orbitals is kept in the catalytic residues Tyr14 and Asp99, and returned to Asp38, as shown in Figure 2b and Figure 3. Thus, the catalytic residues, through SSHBs, play the role of a charge buffer, stabilizing the intermediates by sharing the negative charge built up on the substrate in the course of the reaction. This lowers the HOMO energy level, as shown in Figure 2c, which results in high stabilization of TSs and intermediates. Thus, the lowering of activation barriers in the presence of catalytic residues is well understood from the quantum nature that the excess electron density accumulated on the substrate through deprotonation by Asp38 tends to be dissipated to the catalytic residues for better stabilization. This situation is similar to what is observed in case of an excess electron interacting with solvents (*39, 40*). Thus, the presence of the catalytic residues drastically reduces the charge build-up on the O3 by the charge buffering role. This stabilization, which is highly enhanced in the presence of both Asp99 and Tyr14, is driven by the partial proton transfers and the charge redistributions promoted by SSHBs. Thus, this clear interpretation supports our previous conclusion of the role of catalytic residues in the enzyme reaction (*30*).

Therefore, we reiterate our previous conclusion here. The catalytic residues catalyze the first step by abstracting the proton from the substrate and the third step by donating the proton to the substrate. The first step will be facilitated by acidic residues with a lower proton affinity, while the third step will be facilitated by basic residues with a higher proton affinity. So, the catalytic residues play a dual role in catalysis as proton donor and acceptor alternatively. Thus, in the two-step reaction mechanism of KSI, the SSHBs as amphi-acid/base catalysts, along with the partial proton transfers and electronic charge redistributions, play a crucial role in strongly stabilizing EIs or TS2 (∼15 kcal/mol) and shortening $d(O_3-O_r)$ (down to ∼2.5 Å by ∼0.2 Å) in the apolar active site. The catalytic reactivity of KSI is governed by the SSHBs as amphi-acid/base catalysts which facilitate a change in bond orders (i.e., double bond shifts) of carbon−carbon bonds in the substrate. Thus, the catalytic role of SSHB is attributed to the dual role of proton donor/acceptor (to/from substrate) in catalytic activations of two-step reactions (to be catalyzed alternatively by acid and base), as the partial proton shuttles and electron rearrangements are driven by SSHB. A large stabilization energy for EIs/TSs relative to ES comes from both the enhanced H-bonds (SSHBs) energy (i.e., mostly electrostatic energy) and the molecular orbital interaction energy due to the charge redistributions (associated with a change in bond order in the substrate) involved in electron dissipation to the catalytic residues. The latter interaction energy includes induction energy related to the charge transfer and polarizability. The preorganized induced polarization energy (promoted by SSHB) would be considered as extended preorganization energy which stabilizes EIs and TSs over ES. This is contrasted to the well-known preorganization energy which is generally considered in terms of both the favorable size matching between an enzyme and a substrate and the electrostatic energy gain of a substrate due to the preorganized dipole moieties (i.e., preorganized orientational polarization) of an enzyme without

structural change of the substrate (*20*). The criticism against SSHB seems to arise mainly from the study of enzymes involving one-step reaction pathway mechanism wherein the SSHB may not be so important (*41*, *42*).

CONCLUDING REMARKS

KSI which is associated with metabolites of bacteria and steroid hormones of mammals has been an exemplary study for fast diffusion-controlled reaction mechanisms in enzymes. Both X-ray structures (of two homologous enzymes in free or in complex with intermediate-like and product-like inhibitors) and extensive ab initio theoretical analysis clearly demonstrate the following. The substrates and inhibitors in the active site are found to have two hydrogen bonds regardless of solution or crystal state. The hydrogen bond lengths between the oxyanion-O3 and the anionic oxygen atoms in the catalytic residues are short (∼2.6 Å) in the presence of intermediate analogues. These distances are shorter than those (∼2.8 Å) of the reactants or products by about ∼ 0.2 Å. The origin of high reactivity is due to the two-step reaction mechanism involving amphi-acid/base roles assisted by SSHB. In this mechanism, high stabilization of the intermediate responsible for the almost diffusion controlled reactivity is due to partial proton transfers and charge redistributions by dissipation of negative charge density built up on substrates. This results in large gains in both electrostatic and induction energies.

REFERENCES

1. Kuliopulos, A., Talalay, P., and Mildvan, A. S. (1990) *Biochemistry 29*, 10271−10280.
2. Xue, L., Kuliopulos, A., Mildvan, A. S., and Talalay, P. (1991) *Biochemistry 30*, 4991−4997.
3. Xue, L., Talalay, P., and Mildvan, A. S. (1991) *Biochemistry 30*, 10858−10865.
4. Holman, C., and Benisek, W. (1995) *Biochemistry 34*, 14245−14253.
5. Wu, Z. R., Ebrahimian, S., Zawrotny, M. E., Thornburg, L. D., Perez-Alvarado, G. C., Brothers, P., Pollack, R. M., and Summers, M. F. (1997) *Science 276*, 415−418.
6. Kim, S. W., Cha, S.-S., Cho, H.-S., Kim, J.-S., Ha, N.-C., Cho, M.-J., Joo, S., Kim, K.-K., Choi, K. Y., and Oh, B.-H. (1997) *Biochemistry 36*, 14030−14036.
7. Cho, H.-S., Choi, G., Choi, K. Y., and Oh, B.-H. (1998) *Biochemistry 37*, 8325−8330.
8. Gerlt, J. A., and Gassman, P. G. (1993) *J. Am. Chem. Soc. 115*, 11552−11568.
9. Zhao, Q., Abeygunawardana, C., Talalay, P., and Mildvan, A. S. (1996) *Proc. Natl. Acad. Sci. U.S.A. 93*, 8220−8224.
10. Kuliopulos, A., Mildvan, A. S., Shortle, D., and Talalay, P. (1989) *Biochemistry 28*, 149−159.
11. Xue, L., Kuliopulos, A., Mildvan, A. S., and Talalay, P. (1991) *Biochemistry 30*, 4991−4997.
12. Xue, L., Talalay, P., and Mildvan, A. S. (1991) *Biochemistry 30*, 10858−10865.
13. Li, Y. K., Kuliopulos, A., Mildvan, A. S., and Talalay, P. (1993) *Biochemistry 32*, 1816−1824.
14. Zhao, Q., Abeygunawardana, C., Gittis, A. G., and Mildvan, A. S. (1997) *Biochemistry 36*, 14616−14626.
15. Petrounia, I. P., and Pollack R. M. (1998) *Biochemistry 37*, 700−705.
16. Cho, H. S., Ha, N. C., Choi, G., Kim, H. J., Lee, D., Oh, K. S., Kim, K. S., Lee, W., Choi, K. Y., and Oh, B. H. (1999) *J. Biol. Chem. 274*, 32863−32868.
17. Hibbert, F., and Emsley, J. (1990) *Adv. Phys. Org. Chem. 26*, 255−379.
18. Emsley, J. (1980) *Chem. Soc. Rev. 9*, 91−124.
19. Cleland, W. W., and Kreevoy, M. M. (1994) *Science 264*, 1887−1890.
20. Cleland, W. W., Frey, P. A., and Gerlt, J. A. (1998) *J. Biol. Chem. 273*, 25529−25532.
21. Warshel, A. (1998) *J. Biol. Chem. 273*, 27035−27038.
22. Canon, W. R., and Benkovic, S. J. (1998) *J. Biol. Chem. 273*, 26257−26260.
23. Shan, S., and Herschlag, D. (1996) *Proc. Natl. Acad. Sci. U.S.A. 93*, 14474−14479.
24. Frey, P. A., Whitt, S. A., and Tobin, J. B. (1994) *Science 264*, 1927−1930.
25. Zhao, Q., Abeygunawardana, C., Talalay, P., and Mildvan, A. S. (1996) *Proc. Natl. Acad. Sci. U.S.A. 93*, 8220−8224.
26. Loh, S. N., and Markley, J. L. (1994) *Biochemistry 33*, 1029−1036.
27. Thornburg, L. D., Henot, F., Bash, D. P., Hawkinson, D. C., Bartel, S. D., and Pollack, R. M. (1998) *Biochemistry 37*, 10499−10506.
28. Massiah, M. A., Abeygunawardana, C., Gittis, A. G., and Mildvan, A. S. (1998) *Biochemistry 37*, 14701−14712.
29. Zhao, Q., Beygunawardana, C., Talalay, P., and Mildvan, A. S. (1997) *Biochemistry 36*, 3458−3472.
30. Kim, K. S., Oh, K. S., and Lee, J. Y. (2000) *Proc. Natl. Acad. Sci. U.S.A. 97*, 6373−6378.
31. Kim, S. W., and Choi, K. Y. (1995) *J. Bacteriol. 177*, 2602−2605.
32. Kim, S. W., and Choi, K. Y. (1995) *Mol. Cells 5*, 354−358.
33. Hawkinson, D. C., Pollack, R. M., and Ambulos, N. P., Jr. (1994) *Biochemistry 33*, 12172−12183.
34. Otwinoski, Z., and Minor, W. (1997) *Methods Enzymol. 276*, 307−326.
35. Brunger, A. T. (1992) *X-PLOR*, Version 3.0, Yale University Press, New Haven, CT.
36. Frisch, M. J. (1995) *Gaussian 94*, Gaussian, Inc., Pittsburgh, PA.
37. Kim, S. W., Joo, S., Choi, G., Cho, H.-S., Oh, B.-H., and Choi, K. Y. (1997) *J. Bacteriol. 179*, 7742−7747.
38. Hawkinson, D. C., Eames, C. M., and Pollack, R. M. (1991) *Biochemistry 31*, 10849−10858.
39. Lee, S., Kim, J., Lee, S. J., and Kim, K. S. (1997) *Phys. Rev. Lett. 79*, 2038−2041.
40. Majumdar, D., Kim, J., and Kim, K. S. (2000) *J. Chem. Phys. 112*, 101−105.
41. Smith, D. M., Golding, B. T., and Radom, L. (1999) *J. Am. Chem. Soc. 121*, 1383−1384.
42. Chen, J., McAllister, M. A., Lee, J. K., and Houk, K. N. (1998) *J. Org. Chem. 63*, 4611−4619.

BI001629H